

Morphological Parameters in Varieties of Silk Fibers Determined by Small-Angle X-ray Scattering

J. DAVID LONDONO,¹ V. ANNADURAI,² R. GOPALKRISHNE URS,³ R. SOMASHEKAR⁴

¹ Dupont Central Research, E.I. Dupont de Nemours and Company, Experimental Station, Wilmington, DE 19880-0323

² Department of Physics, BIET, Davanagere 577 004, India

³ Department of Applied Physics, NIE, Mysore 570 008, India

⁴ Department of Studies in Physics, University of Mysore, Manasagangotri Mysore-570 006, India

Received 17 August 2000; accepted 17 September 2001

ABSTRACT: The small-angle X-ray scattering intensity data recorded from silk fibers were compared with the simulated data obtained from a linear paracrystalline model. For this purpose, an exponential distribution function for the amorphous and crystalline phase lengths was used. There are significant changes in phase lengths because of amino acid compositional changes in different families of silk fibers. © 2002 Wiley Periodicals, Inc. *J Appl Polym Sci* 85: 2382–2388, 2002

Keywords: silk fibers; small-angle X-ray scattering (SAXS); phase lengths

INTRODUCTION

Silk, a fibrous protein, is an important textile material. Natural polymers, like silk fibers, have both crystalline (ordered) and amorphous (disordered) regions due to the presence of long and flexible molecular chains that hinder further crystallization.¹ The distribution and size of the crystalline and amorphous regions of fibers influence the physical properties of the material. Silk has been shown to be of a linear paracrystalline^{2–4} nature. Marsh et al.⁵ reported on the crystal structures of *Bombyx mori* and Tassar fiber,⁶ a wild variety belonging to *Antheraea* family. In the *Bombyx mori* and *Antheraea* families of silk fibers, the crystalline fraction mainly contains the amino acid residues, glycine, alanine, and

serine.² The molecular chain axis in the crystals and the long axis of the stacks aligned along the fiber have been reported by Grubb and Gending.⁷ The effect of elongation in silk fibers on the small-angle X-ray scattering (SAXS) pattern has been investigated by Hirabayashi.⁸ An attempt has been made recently⁹ to remove the ambiguity about the small-angle X-ray scatter from silk fibers belonging to the *Bombyx mori* family by combined atomic force microscopy (AFM) and SAXS studies.

Until now, SAXS studies of silk fibers have been lacking because of poor scattering. In this report, we compare the SAXS patterns of different varieties of silk fibers belonging to the *Bombyx mori* and *Antheraea* families that were determined with synchrotron radiation of wavelength 1.541 Å. These results are compared with those from a two-phase model incorporating a statistical variation in the lengths of crystalline and amorphous regions as well as distortion effects within crystallites.

Correspondence to: R. Somashekar (rsshekar@sanchernet.in or rs@uomphysics.net).

Journal of Applied Polymer Science, Vol. 85, 2382–2388 (2002)
© 2002 Wiley Periodicals, Inc.

Table I Characteristic Physical Properties of Silk Fibers

Sample (Race)	Family	Shape of Cocoon	Cocoon Color	Fiber Color	Average Filament Length, m	Denier	Lifecycle per Year	Tensile Strength, MPa	Elongation at break, %
PMS	<i>Bombyx mori</i>	Spindle	Light green	Light green	350	1.8–2	6 (generation) Multivoltine (MV)	258 ± 22	36 ± 4
Temp. BV	<i>Bombyx mori</i>	Dumple/oval	White	White	1050	2.4–2.8	2 Bivoltine (BV)	219 ± 35	33 ± 1
Nistari	<i>Bombyx mori</i>	Spindle	Pink	Pink	340	1.8–2	6 MV	284 ± 51	22 ± 2
HM	<i>Bombyx mori</i>	Oval	Dark green	Light green	550	2	6 MV	340 ± 26	33 ± 4
Muga	<i>Antheraea</i>	Oblong	Golden brown	Golden yellow	350–450	4.5–5	5–6 MV	175 ± 12	27 ± 1
Tassar	<i>Antheraea</i>	Oval	Yellow/gray	Light brown	600–1400	7–14	6–7 MV	236 ± 17	24 ± 1

EXPERIMENTAL

Sample Preparation

Cocoons of the silk worm (*Bombyx mori* and *Antheraea* families) are the raw product used to reel silk fibers. Cocoons of *Bombyx mori* family include (1) pure Mysore silk (PMS), (2) temperate Bivoltine (temp. BV), (3) Nistari, and (4) hosa Mysore (HM), and cocoons of wild silk worms belonging to the *Antheraea* family include (5) Muga and (6) Tassar. These cocoons were collected from the germplasm stock and were reeled according to the standard procedure. First, cocoons were cooked in boiling water for 2 min to soften the sericin and then they were transferred to a water bath at 65 °C for 2 min. Next, the cocoons were reeled in warm water with reeling equipment (Epprouvite; M/s S R Enterprises, Government of India, Bangalore, India). The mechanical properties, such as tensile strength and percentage of elongation at break, were measured according to the ASTM D-882 method using a Hounsfield Universal Testing Machine (UTM). The characteristic physical properties of these silk fibers, reported as means and standard deviations of six sampled, are given in Table I. The sample cross section varied from 0.09 to 0.83 mm². Tensile strength was determined from the ratio of maximum normal load to the cross-sectional area. A summary of essential physical features of silk fibers used in this study is given in Table I.

SAXS Recording

The SAXS recordings were performed at the DND-CAT Synchrotron Research Center, Advanced Photon Source, Argonne National Laboratory. The energy of the X-ray beam from an insertion device (ID) was adjustable from 7 to 18 KeV. The ID; double crystal monochromator; first, second, and third sets of adjustable slits; and the sample were located at 0, 30, 35, 54, 66, and 68 m, respectively, along the X-ray beam path from the synchrotron orbit. The size of the square beam was defined at the first and second sets of the slits, which were both set at 100 μm. A parasitic scattering slit, with a round pinhole shape only large enough to circumscribe the square beam, was placed 1–2 mm before the sample. The 2-D CCD (Mar) detector, with 2048 × 2048 pixels with a 16-bit intensity scale and a circular active area of 133 mm diameter, was used. In all cases, the detector was used in a 4 × 4 binning mode at a

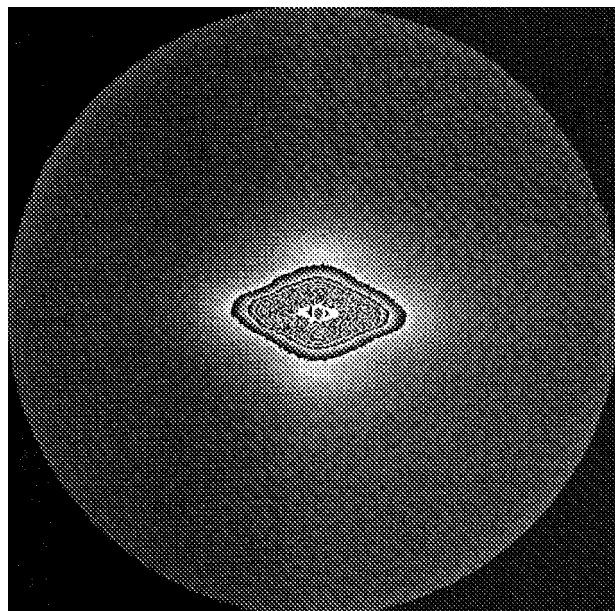


Figure 1 The SAXS pattern for Muga silk fibers with an exposure period of 10 s.

resolution of 512×512 , with an effective pixel size of $258 \mu\text{m}/\text{pixel}$. The detector was placed at the end of an evacuated 8-inch pipe fitted with Kapton® windows on both ends. The sample-to-detector distance was adjustable from a few centimeters to 8.5 m. The detector was placed at a distance of 722 mm away from the sample, and the ID was tuned to an energy of 8.048 KeV, corresponding to the wavelength 1.541 \AA . At this distance, the detector covered scattering angles 2θ corresponding to the range in the scattering vector magnitudes $5 \times 10^{-3} < q (= 4\pi \sin\theta/\lambda) < 4 \times 10^{-1} \text{ \AA}^{-1}$. The recordings were carried out for a 10-s exposure time and without sample, air scattering data were collected for a known interval of time, and then the scattering data at higher q values were normalized with the sample scattering data and then subtracted from the sample data. The SAXS pattern for the silk fiber Muga; using an exposure period of 10 s is shown in Figure 1.

Analysis and Computation

Quasi-periodic alternation of electron density in polymer fibers has been investigated by SAXS studies.^{10,11} It is now well established that the structure contains stacks in which crystalline lamellae are separated by less dense regions. Hosemann and Bagchi¹² have obtained the following relations:

$$I_B(s) = \frac{\Delta\rho^2 N}{(2\pi s)^2} \left\{ \frac{|1 - H_y|^2(1 - |J_z|^2) + |1 - J_z|^2(1 - |H_y|^2)}{|1 - H_y J_z|^2} \right\} \quad (1a)$$

$$I_c(s) = \frac{\Delta\rho^2}{2(\pi s)^2} \text{Re} \left\{ \frac{J_z(1 - H_y)^2(1 - (H_y J_z)^N)}{(1 - H_y J_z)^2} \right\} \quad (1b)$$

$$I(s) = I_B(s) + I_c(s) \quad (1c)$$

where $I(s)$ is the intensity of scattering, by a paracrystal entity such as that just described, as a function of s ($s = 2\sin\theta/\lambda$), where 2θ is the scattering angle and λ is the wavelength of the radiation; (H_y, J_z) is the Fourier transforms of the normalized distribution function of the lengths of the units of the two phases; N is the number of repeating units in the paracrystal; and $\Delta\rho$ is the difference between the electron densities of the phases.

In the present work, eq. 1 is developed into a form that is easier to compute in terms of exponential distribution function for the two phase lengths in silk fibers.

It has been shown¹³⁻¹⁵ that eq. 1 can be reduced to:

$$\frac{2I(\pi s)^2}{\Delta\rho^2} = \frac{C}{F} + \frac{D + E}{F^2} \quad (2a)$$

where

$$F = 1 + A^2 B^2 - 2AB \cos X \quad (2b)$$

$$C = N\{1 - A^2 B^2 - A(1 - B^2)\cos\phi - B(1 - A^2)\cos\chi\} \quad (2c)$$

$$D = B[(1 - A^2)(1 - A^2 B^2)\sin X \sin\phi + \{(1 + A^2 B^2)\cos X - 2AB\}\{(1 + A^2)\cos\phi - 2A\}]/G \quad (2d)$$

$$G = 1 - A^N B^N \cos NX \quad (2e)$$

$$E = A^N B^{N+1} \sin NX [(1 - A^2 B^2)\{(1 + A^2)\cos\phi - 2A\}\sin X - (1 - A^2)\{(1 + A^2 B^2)\cos X - 2AB\}\sin\phi] \quad (2f)$$

by taking

$$H_y = A \exp(-i\chi) \quad (3a)$$

$$J_z = B \exp(-i\phi) \quad (3b)$$

and

$$X = \chi + \phi \quad (3c)$$

where X is the distribution width. We used an exponential distribution function for the phase lengths because it gives fairly reliable results in wide-angle X-ray scattering (WAXS) studies of polymer fibers.¹⁶ The normalized exponential distribution function is given by

$$h(x) = \alpha \exp(-\alpha(x - \varepsilon)) \quad (4)$$

where $\alpha = (1/2\gamma)$, $\langle Y \rangle$; $\varepsilon = \langle Y \rangle(1 - 2\gamma)$; and γ is a parameter controlling both the skew and the dispersion of the distribution. Provided $0 < \gamma < 0.5$, lengths less than ε are not possible because this situation would cause $h(x)$ to be negative. By taking the Fourier transform of this function (eq. 4), we get

$$A = \frac{1}{(1 + 4\pi^2 s^2 \gamma_y^2 \langle Y \rangle^2)^{1/2}} \quad (5)$$

$$\chi = s\varepsilon_y + \cos^{-1} \left[\frac{1}{(1 + 4\pi^2 s^2 \gamma_y^2 \langle Y \rangle^2)^{1/2}} \right] \quad (6)$$

Similar equations for B and ϕ are given by

$$B = \frac{1}{(1 + 4\pi^2 s^2 \gamma_z^2 \langle Z \rangle^2)^{1/2}} \quad (7)$$

$$\phi = s\varepsilon_z + \cos^{-1} \left[\frac{1}{(1 + 4\pi^2 s^2 \gamma_z^2 \langle Z \rangle^2)^{1/2}} \right] \quad (8)$$

Thus, with the exponential distribution for each phase, we have A , B , χ , and ϕ which can be used in eq. 2, and the intensity can be calculated as a function of s using the parameters describing the distribution. Here, suffixes y and z refer to the two phases present in the polymers. The model also incorporates the statistical variation of defects in the crystallites.

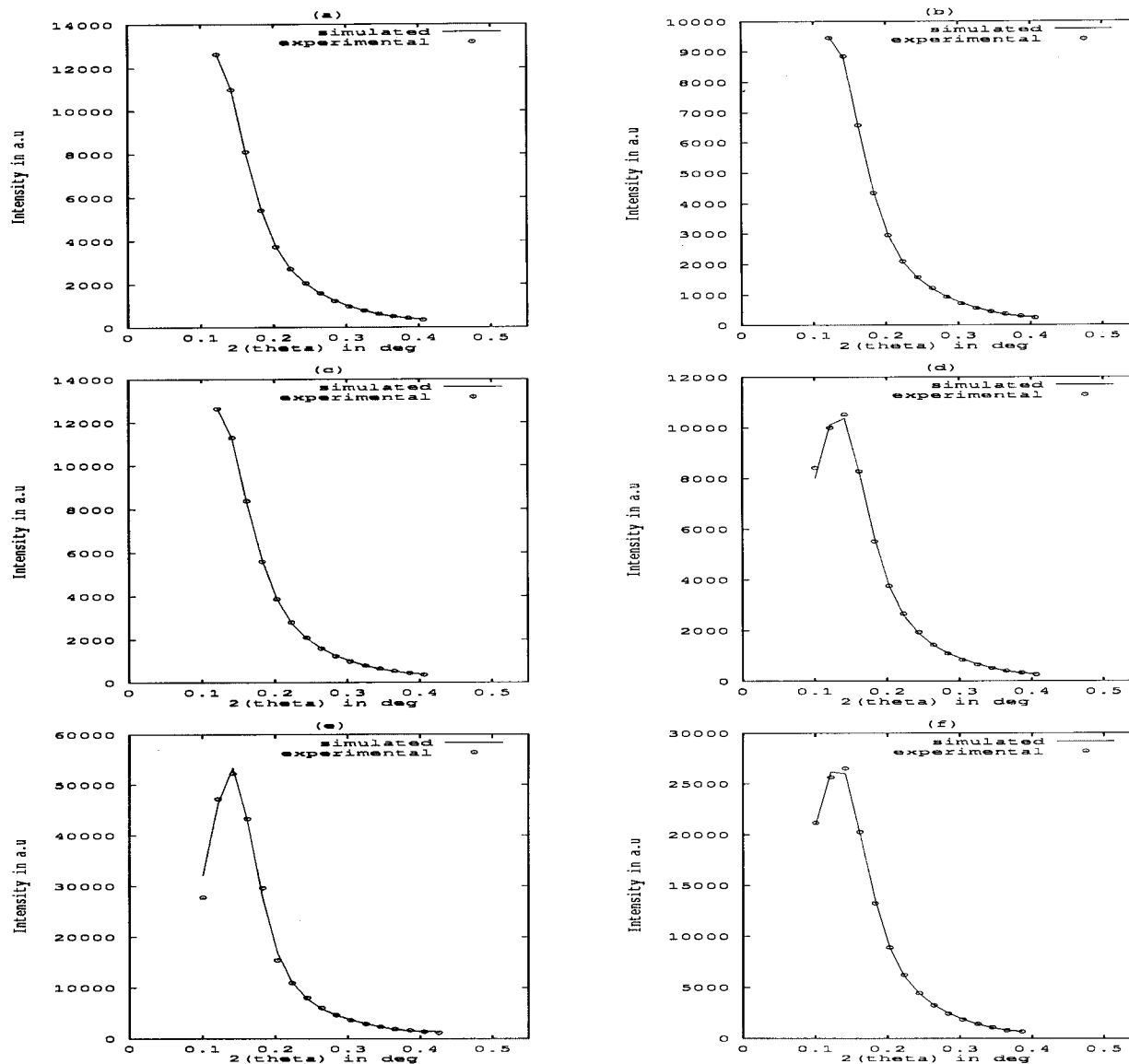
To test the model just described, we used SAXS data from a variety of silk fibers. From eqs. 2, 5, and 6, and the intensity data, it is possible to determine the periodicity ($\langle Y \rangle + \langle Z \rangle$), where $\langle Y \rangle$ and $\langle Z \rangle$ are the mean lengths of the two phases, the phase ratio ($\langle Y \rangle / [\langle Y \rangle + \langle Z \rangle]$); the two param-

eters defining the widths of the distribution functions of the lengths of the phases; and the number of units (N) in the paracrystal. To find the combinations of these that will give the best fit to the experimental data for an exponential distribution function, a stepping refinement procedure minimizing the sum of χ^2 over all data points was used.

RESULTS AND DISCUSSION

The best fit between experimental results and simulated profile (10 s) was obtained with an exponential distribution function for all the samples, as shown in Figure 2. A good fit to the experimental data is observed for a range of scattering angles (2θ) between 0.1 and 0.5°. The normalized exponential probability distribution functions of phase lengths (crystalline and amorphous) for this model, shown in Figure 3, are obtained from the model parameters given in Table II and by employing eq. 4 for the two phases Y and Z . The results displayed in Figures 3(a) and 3(b) demonstrate corresponding changes in the distribution of phase lengths along the fiber axis of different varieties of silk fibers. The small changes in morphological parameters, like crystalline and amorphous phase length, are due to the composition of amino acids in the *Bombyx mori* and *Antheraea* families. Note that alanine, glycine, and serine residues are present at 29, 45, and 12%, respectively, in the *Bombyx mori* family, and at 41, 27, and 11%, respectively, in *Antheraea* family. Also, along the fiber axis in the *Bombyx mori* family, fibroin, alanine, and glycine residues are located on either side of the helical axis. The atomic coordinates of serine, which are the same as those of alanine except for its oxygen atom are located in the neighborhood of those of alanine.

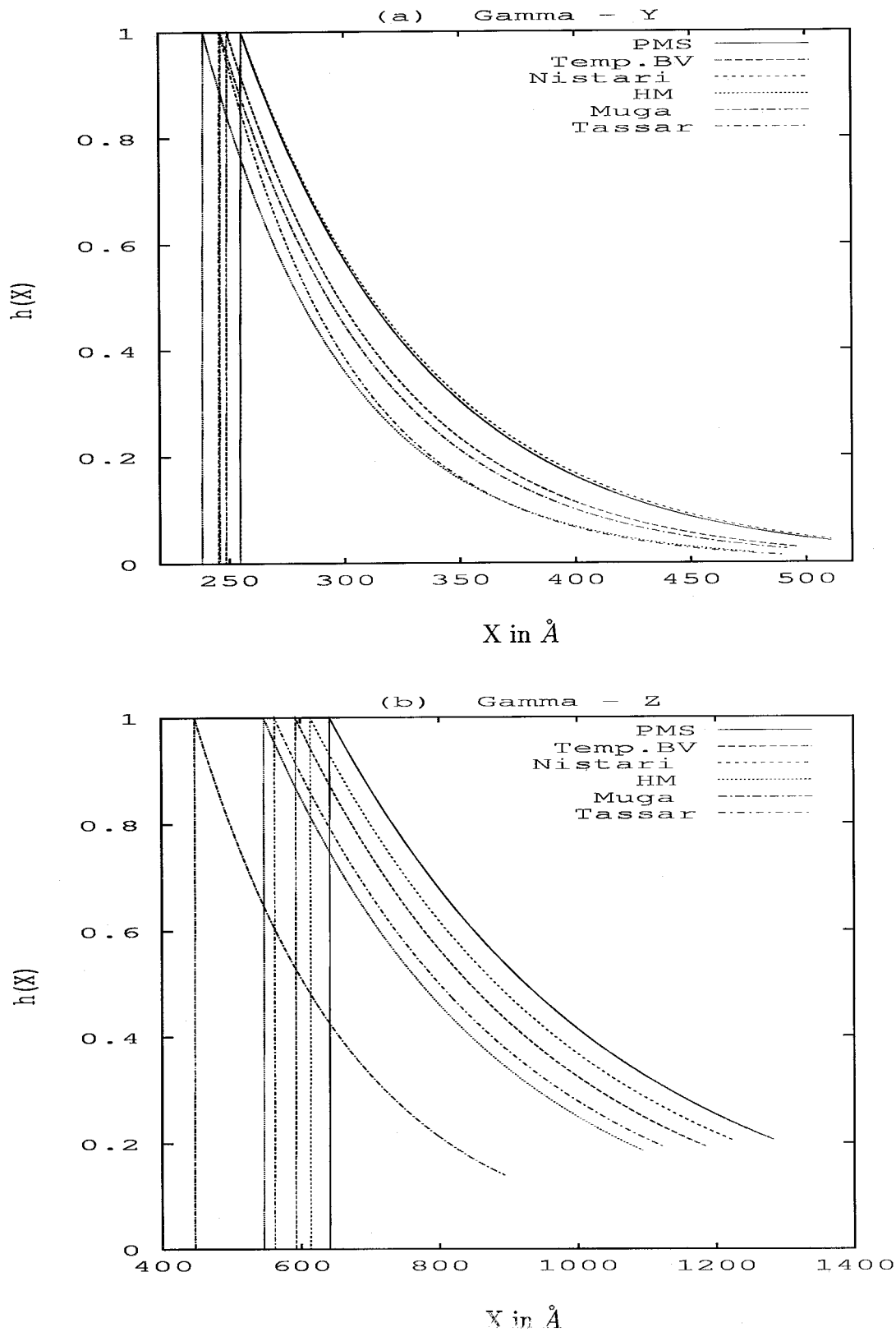
In silk fibers (like Muga and Tassar) belonging to the *Antheraea* family, there is insufficient glycine to allow alternating of chains to any considerable extent. However, there is efficient interlocking of the side chains of adjacent sheets in both *Bombyx mori* and *Antheraea* families of silk fibers. The structures of all the fibroins are related to the antiparallel chain pleated sheets, and the differences in the structure are mainly in the spacing of these sheets, which are determined by the sizes of the side chains of the amino acids that comprise the sheets. These microstructural aspects justify the observed results; that is, there is not much change in the width and shape of the



Figures 2 The experimental and simulated SAXS profile of silk fibers belonging to the *Bombyx mori* family [(a) pure Mysore silk, (b) temperate Bivoltine, (c) Nistari, and (d) Hosa Mysore] and to the *Antheraea* family [(e) Muga and (f) Tassar].

function gamma-Y (γ_y ; amorphous region), but a very small change is observed in the width and shape of the function gamma-Z (γ_z ; crystalline region). It is evident from the results in Table II that the periodicity ($\langle Y \rangle + \langle Z \rangle$) and the widths of the distribution functions gamma-Y and gamma-Z are higher in PMS and lower in Muga fibers. This difference is attributed to the higher percentage of alanine residues in silk fibers belonging to the *Bombyx mori* family. These observations are further justified by the results of the tensile strength and percentage of elongation in

silk fibers; that is, there is not much significant variation in these parameters. The changes observed in amorphous and crystalline lengths within the *Bombyx mori* family of silk fibers arise not only because of organizational changes of β -pleated structures along the length of the fibers, but also because of unfolding of the molecular chains.¹⁷ Here, the crystalline phase length is given by $\langle Z \rangle$, which has a higher value than the amorphous phase length $\langle Y \rangle$. This result is consistent with the observation of Meyer et al.¹⁸ that the amino acid sequence scheme in the crystalline



Figures 3 The normalized exponential probability distribution functions of the lengths of the amorphous and crystalline phases.

Table II Values of Morphological Parameters for *Bombyx mori* and *Antheraea* Families of Silk Fibers

Sample	Periodicity, Å	Phase Ratio	γ_y	γ_z	$\langle Y \rangle$, Å	$\langle Z \rangle$, Å	(χ^2)
Pure Mysore Silk	897.3	0.285	0.155	0.316	255.4	641.9	0.55
Temperate Bivoltine	841.3	0.296	0.139	0.304	248.7	592.6	0.64
Nistari	869.8	0.294	0.158	0.313	255.6	614.2	0.60
Hosa Mysore	786.2	0.304	0.125	0.297	238.9	547.3	1.78
Muga	694.2	0.355	0.135	0.253	246.3	447.9	9.99
Tassar	808.5	0.304	0.115	0.303	245.7	562.8	4.21

region is G A G A G S G A G A G A and that in the amorphous region is G T Ar G (where G is glycine, A is alanine, T is tyrosine, S is serine, and Ar is arginine).

CONCLUSIONS

The simulated SAXS patterns from a Hosemann's linear paracrystalline model for several varieties of silk fibers agree very well with the experimental data. The changes in morphological parameters are due to compositional as well as organizational differences in the amino acids of silk fibers belonging to the *Bombyx mori* and *Antheraea* families.

The authors thank the CSIR and UGC, New Delhi, for the financial assistance and JSPS for a visiting fellowship (RS), the UGC, New Delhi, for financial assistance (RGK), and the BIET, Davanagere, for encouragement (VA).

REFERENCES

- Somashekar, R.; Gopalkrishne Urs, R. *Pramana J Phys* 1993, 40, 335.
- Warwicker, J. O. *J Molec Biol* 1960, 2, 350.
- Bhat, N. V.; Karlekar, R. B.; Chitra, N.; Geetha, P. In *Proceedings of the Polymer Conference; Research Centre, IPCL, Baroda, India, 1994*.
- Ambrose, E. J.; Elliott, A. *Proc R Soc. London, Ser A* 1951, A206, 206.
- Marsh, R. E.; Corey, R. B.; Pauling, L. *Biochim Biophys Acta* 1955, 16, 1.
- Marsh, R. E.; Corey, R. B.; Pauling, L. *Acta Crystallogr* 1955, 8, 710.
- Grubb, D. T.; Gending Ji. *Int J Biol Macromol* 1999, 24, 203.
- Nobumasa Hojo. *Structure of Silk Yarn Vol. I; Oxford & IHB Publishing: New Delhi, India, 2000; p. 227*.
- Miller, L. D.; Putthanarat, S.; Eby, R. K.; Adams, W. W. *Int J Biol Macromol* 1999, 24, 159.
- Blundel, D. J. *Polymer* 1978, 19, 1258.
- Crist, B.; Morosoff, N. *J Polym Sci Polym Phys* 1973, 11, 1023.
- Hosemann, R.; Bagchi, S. N. *Direct Analysis of Diffraction by Matter; Elsevier/North Holland: New York, 1962*.
- Hall, I. H.; Mahmood, E. A.; Carr, P. D.; Geng, Y. D. *Coll Polym Sci* 1987, 265, 383.
- Hall, I. H.; Toy, M. Hall, I. H. In *Structure of Crystalline Polymers; Hall, I. H.; Ed.; Elsevier Applied Science: New York, 1984; p. 181*.
- Annadurai, V.; Gopalkrishne Urs, R.; Siddaramaiah; Somashekar, R. *Polymer* 2000, 41, 5689.
- Somashekar, R.; Somashekarappa, H. *J Appl Crystallogr* 1997, 30, 147.
- Iizuka, E., *Experientia* 1983, 39, 449.
- Meyer, K. H.; Flud, M.; Klemm, O., *Helv Chim Acta* 1940, 22, 22.